COMPLEX SYSTEM MODELING AND SIMULATION
ISSN 2096-9929 03/06 pp 142−155
Volume 2, Number 2, June 2022
DOI: 10.23919/CSMS.2022.0008

A Region Enhanced Discrete Multi-Objective Fireworks Algorithm for Low-Carbon Vehicle Routing Problem

Xiaoning Shen, Jiaqi Lu, Xuan You, Liyan Song*, and Zhongpei Ge

Abstract: A constrained multi-objective optimization model for the low-carbon vehicle routing problem (VRP) is established. A carbon emission measurement method considering various practical factors is introduced. It minimizes both the total carbon emissions and the longest time consumed by the sub-tours, subject to the limited number of available vehicles. According to the characteristics of the model, a region enhanced discrete multi-objective fireworks algorithm is proposed. A partial mapping explosion operator, a hybrid mutation for adjusting the sub-tours, and an objective-driven extending search are designed, which aim to improve the convergence, diversity, and spread of the non-dominated solutions produced by the algorithm, respectively. Nine low-carbon VRP instances with different scales are used to verify the effectiveness of the new strategies. Furthermore, comparison results with four state-of-the-art algorithms indicate that the proposed algorithm has better performance of convergence and distribution on the low-carbon VRP. It provides a promising scalability to the problem size.

Key words: vehicle routing problem; carbon emission; multi-objective optimization; fireworks algorithm; region enhanced

1 Introduction

In response to the strategy of global sustainable development, logistics companies have started paying attention to the environmental benefits of logistics activities while improving economic incomes, and the concept of "green logistics" emerged at the historic moment[1]. At present, the impact of logistics on the environment is mainly reflected in the increase of the greenhouse gas emissions such as carbon dioxide, which pollutes the atmospheric environment and accelerates global warming and climate destruction[2]. In order to improve this phenomenon, different enterprises are beginning to pay attention to green logistics. In the cold chain transportation industry, Zulvia et al.[3] established a low-carbon vehicle routing problem (VRP) model considering the carbon emissions and the product quality, which is applicable to enterprises that sell perishable products such as fruits, vegetables, and flowers. In the waste collection industry, Jabbarzadeh et al.[4] proposed a waste collection model that minimizes the traveling cost, greenhouse gas emissions, and the energy consumption and applied it to a practical case of Tehran municipal solid waste collection. In the electric vehicles charging industry, Long and Jia[5] developed a bi-level Q-learning to solve the stochastic matching of renewable

• Xiaoning Shen is with the Collaborative Innovation Center of Atmospheric Environment and Equipment Technology, Jiangsu Key Laboratory of Big Data Analysis Technology, School of Automation, Nanjing University of Information Science and Technology, Nanjing 210044, China. E-mail: sxnystsyt@sina.com.
• Jiaqi Lu, Xuan You, and Zhongpei Ge are with the School of Automation, Nanjing University of Information Science and Technology, Nanjing 210044, China. E-mail: 1229365885@qq.com; 563752923@qq.com; 965159334@qq.com.
• Liyan Song is with the Research Institute of Trustworthy Autonomous Systems, and also with the Guangdong Provincial Key Laboratory of Brain-Inspired Intelligent Computation, Department of Computer Science and Engineering, Southern University of Science and Technology, Shenzhen 518055, China. E-mail: songly@sustech.edu.cn.
∗ To whom correspondence should be addressed.
Manuscript received: 2022-01-11; revised: 2022-05-01; accepted: 2022-05-18

power generation and electric vehicles charging demand, which reduces the carbon emissions and the charging cost. These problems aim at reducing the carbon emissions produced by vehicles during transportation. Transportation is the main component and core link of logistics activities. If all the transport carriers are regarded as vehicles, logistics transportation can be regarded as a vehicle routing problem[6]. VRP is a classical combinatorial optimization problem, from which different types of VRP are derived, and the low-carbon VRP is one of them. In order to reduce the emissions of greenhouse gases and improve the quality of the atmospheric environment, the low-carbon VRP has become a popular research topic of combinatorial optimization for the past few years.

Since the notion of low-carbon VRP was first introduced, many researchers have studied on the modeling and the solution of this problem, and achieved gratifying results. In recent works on modeling the low-carbon VRP, multiple objectives, like carbon emission, cost, and travel time, are simultaneously considered in most of the existing researches. Jemai et al.[7] established a mathematical model which aims at minimizing both the carbon emissions and the total driving distance, and adopted non-dominated sorting genetic algorithm II (NSGA-II)[8] to solve the model. Xu et al.[9] built a green vehicle routing model with time-varying speed and soft time window, which considered vehicle capacity, time-varying speed, and traffic congestion. Zhang et al.[10] aggregated the vehicle fuel cost, the carbon emission cost, and the vehicle usage cost into one objective. Xiao et al.[11] constructed a fuel consumption vehicle routing model minimizing the vehicle fixed cost and fuel consumption cost. Wang et al.[12] proposed a bi-objective model with real-time load and speed to minimize the total carbon emission and the operating cost. As above, most of the existing low-carbon VRP models take the cost and carbon emissions generated in the transportation as optimization objectives, and almost ignore the optimization of transportation time, which is not suitable for the scene with high requirements on transportation time.

Low-carbon VRP is a non-deterministic polynomial hard (NP-hard) problem[13], and the metaheuristic method is an ideal tool for solving this type of problem[14–20]. For example, Han et al.[15] adopted an improved iterated greedy algorithm to solve the distributed flow shop scheduling problem with sequence-dependent setup time. Zhang et al.[17] designed a multi-direction update based multi-objective particle swarm optimization for mixed no-idle flow-shop scheduling problem. Therefore, more and more metaheuristic algorithms are applied to low-carbon VRP. De Oliveira Da Costa et al.[21] adopted a genetic algorithm (GA) to solve green VRP model, which reduces carbon emissions effectively in the transportation. Zhang et al.[22] designed an improved particle swarm optimization to optimize vehicle transportation costs and carbon emissions in the low-carbon VRP. Pulido-Gaytan et al.[23] designed a multi-objective cellular genetic algorithm, which simultaneously minimized the three objectives of total vehicle travel time, carbon emissions, and environmental penalty costs related to the low-carbon VRP. Li et al.[24] applied an ant colony algorithm incorporating an improved pheromone updating method to the multi-depot vehicle routing problem, which maximizes revenue and minimizes cost, travel time, and carbon emissions simultaneously. Jabir et al.[25] designed an ant colony algorithm based on metaheuristic to solve the multi-depot green vehicle routing model with the objective of minimizing the economic cost and emission cost reduction.

Although some metaheuristic methods have been adopted for solving the low-carbon VRP, some problems still exist to be handled, e.g., low accuracy of the result and insufficient use of the problem-specific information. To cover shortages of the existing methods, fireworks algorithm is studied in this paper to solve low-carbon VRP. Fireworks algorithm[26] is a metaheuristic algorithm first presented by Professor Tan Ying of Peking University in 2010. The fireworks algorithm is inspired by the natural phenomenon that fireworks explode in the night sky to generate sparks and illuminate the surrounding area. Each firework is regarded as a solution in the decision space of the optimization problem, and the explosion of a firework to generate a certain number of sparks can be considered to be the process of searching its neighborhood. Due to its characteristics of instantaneity, simplicity, emergence, distributed parallelism, and diversity, the fireworks algorithm has been successfully applied to protein network functional module detection[27], traffic flow prediction[28], multi-region power system scheduling[29], and other realworld problems. So far, there have been some studies on multi-objective optimization fireworks algorithms (MOFWAs). Zheng et al.[30] firstly applied a fireworks algorithm to the multi-objective optimization problem. Liu et al.[31] proposed an MOFWA which used S-Metric as the fitness evaluation index to significantly improve the diversity. Bejinariu et al.[32] adopted the weighted sum method to transform a multi-objective optimization problem into a single-objective optimization problem. Chen et al.[33] proposed a hybrid multi-objective optimization algorithm based on the multi-objective evolutionary algorithm based on decomposition (MOEA/D) framework, which integrated both the fireworks explosion operator and the mutation strategy. Zhang et al.[34] modified the method to calculate the fireworks explosion radius according to the number of iterations. They also gave an improved method to update the binary encodings, and proposed an MOFWA for the multi-objective software and hardware division.

A constrained multi-objective optimization model for the low-carbon VRP is constructed in this paper, where a carbon emission measurement approach considering various practical factors is introduced. Then a region enhanced discrete multi-objective fireworks algorithm (REDMOFWA) is proposed to settle the established model, which includes three novel strategies. First, in order to enhance the global search of the decision space and the local mining of the region around the fireworks, a partial mapping explosion operator is designed. Second, to maintain the population diversity and avoid the algorithm jumping into the local optimum, a hybrid mutation operator is devised to adjust the sub-tours. Third, with the aim of increasing the solution accuracy of the algorithm and extend the spread of the Pareto front, an objective-driven extending search operator is given. Effectiveness of the new strategies is validated by nine VRP instances with different scales. Compared with four state-of-the-art algorithms, the proposed algorithm has better convergence and distribution performance on the low-carbon VRP.

The remainder of this paper is organized as follows. Section 2 constructs the constrained multi-objective optimization model of the low-carbon VRP. Section 3 describes the proposed region enhanced discrete multi-objective fireworks algorithm for solving the established model. In Section 4, experimental studies are carried out. Section 5 draws the conclusion.

2 Constrained Multi-Objective Optimization Model of Low-Carbon VRP

The multi-objective optimization problem requires that there are some conflicts among multiple objectives, and no solution that can simultaneously optimize all the objectives exists. In this paper, the low-carbon VRP is modeled as a constrained multi-objective optimization problem, which minimizes both the total carbon emissions and the longest sub-tour time, subject to the number of available vehicles. When the longest sub-tour time is shorter, it indicates that all the sub-tours consume less time and the customers are evenly dispersed into each sub-tour, so that the number of customers in each sub-tour is smaller. Correspondingly, the number of vehicles actually used becomes larger, leading to the increase of the total carbon emissions generated during the vehicle driving. This shows that there is a conflict between the total carbon emissions of all vehicles and the longest sub-tour time, which can be used as the two objectives of the multi-objective optimization problem.

The constrained multi-objective optimization model of the low-carbon VRP is described as follows: there is a distribution center (numbered zero) and n customer points (numbered from one to n). The demand required by each customer point $i\,(i=1,2,\ldots,n)$ is q_i, and customers can be served by K vehicles. It is assumed that all vehicles are of the same type. The dead weight of each vehicle is w. The capacity is limited to the sum of the demands of all customer points, and the vehicle has a uniform driving speed v_{ij} when driving from the customer i to the customer j $(i,j\in\{1,2,\ldots,n\}, i\neq j)$.

The decision variables are defined as shown in Eqs. (1) and (2):

$$x_{ijk}=\begin{cases}1,\text{if vehicle } k \text{ travels from customer } i \text{ to } j;\\ 0,\text{otherwise}\end{cases} \tag{1}$$

$$y_{ik}=\begin{cases}1,\text{if customer } i \text{ is served by vehicle } k;\\ 0,\text{otherwise}\end{cases} \tag{2}$$

The objective functions and constraints are as follows:

$$\min Z_1 = FE\sum_{k=1}^{K}\sum_{i=0}^{n}\sum_{j=0,j\neq i}^{n}\Big[x_{ijk}d_{ij}(w+l_{ij})(a+g\sin\theta_{ij}+ gC_r\cos\theta_{ij})+x_{ijk}d_{ij}0.5C_dA\rho v_{ij}^2\Big] \tag{3}$$

$$\min Z_2 = \max\left\{\sum_{i=0}^{n}\sum_{j=0,j\neq i}^{n}x_{ijk}\frac{d_{ij}}{v_{ij}}\right\}, k\in\{1,2,\ \ldots, K\} \tag{4}$$

$$\text{s.t.} \sum_{k=1}^{K} y_{ik} = \begin{cases} 1, i = 1, 2, \ldots, n; \\ K, i = 0 \end{cases} \tag{5}$$

$$\sum_{i=0}^{n} \sum_{j=1}^{n} x_{ijk} = y_{jk},\ \forall k \in \{1, 2, \ldots, K\} \tag{6}$$

$$\sum_{i=1}^{n} \sum_{j=0}^{n} x_{ijk} = y_{jk},\ \forall k \in \{1, 2, \ldots, K\} \tag{7}$$

$$\sum_{i \in S, j \in S} x_{ijk} \leqslant |S| - 1,\ \forall k \in \{1, 2, \ldots, K\},$$
$$S \subseteq \{1, 2, \ldots, n\}, 2 \leqslant |S| \leqslant n \tag{8}$$

$$\sum_{k=1}^{K} \sum_{j=1}^{n} x_{ijk} \leqslant K,\ i = 0 \tag{9}$$

where the total carbon emission of all vehicles and the longest sub-tour time is represented by Eqs. (3) and (4), respectively. The carbon emissions generated by vehicle driving on a road section are obtained by the product of the fuel emission parameter FE and the fuel consumption[35]. Here, the influences of driving distance d_{ij}, speed v_{ij}, dead weight w, load l_{ij}, and road conditions on the vehicle fuel consumption are taken into account. In Eq. (3), a is the vehicle acceleration (unit: m/s^2), g is the gravitational acceleration constant (9.81 m/s^2), θ_{ij} denotes the road slope of the section from customer i to customer j, C_r is the rolling resistance coefficient, C_d is the traction coefficient, A is the front surface area of the vehicle (unit: m^2), and ρ indicates the air density (unit: kg/m^3). Equations (5) − (9) are constraint. Equation (5) shows that each customer can only be served by one car. Equations (6) and (7) ensure that when each customer is served, there must be a vehicle driving from a certain place to the customer point and then leaving from the point after finishing serving. Formula (8) is the classical sub-tour elimination constraint which ensures that there is no sub-tour in the driving route of each vehicle. Formula (9) indicates that the number of vehicles departing from the distribution center cannot exceed the number of available vehicles.

3 A Region Enhanced Discrete Multi-Objective Fireworks Algorithm

For the constructed low-carbon VRP model, a region enhanced discrete multi-objective fireworks algorithm called REDMOFWA is proposed. A partial mapping explosion operator, a hybrid mutation for adjusting the sub-tours, and an objective-driven extending search operator are designed to improve the performance of the algorithm.

3.1 Framework of the algorithm

The low-carbon VRP is a combinational optimization problem, and the integer encoding is adopted in the proposed algorithm REDMOFWA. For a problem with n customers (numbered from one to n), the encoding of each individual is a sequence composed of $0-n$. When decoding, the sequence between two adjacent distribution centers (numbered zero) is the driving route of one vehicle, ensuring that each customer is visited only once by one vehicle. In addition, there is no other sub-tour in the driving route of each vehicle. As a result, all the decoded solutions are feasible, and the problem is transformed into an unconstrained combinatorial optimization problem. The flow-chart of REDMOFWA is shown in Fig. 1, which mainly consists of six components: (1) initialization; (2) partial

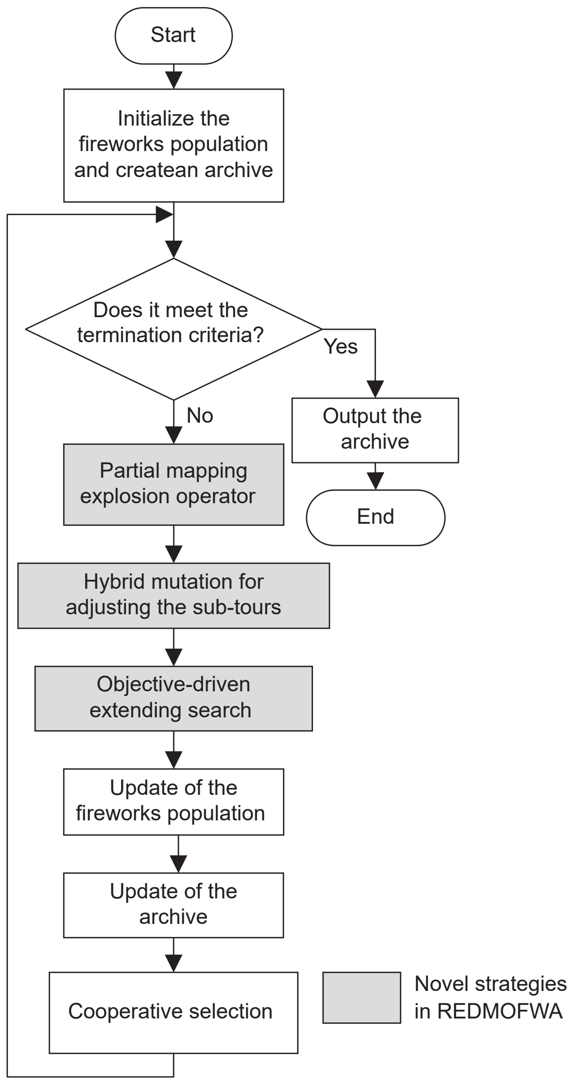

Fig. 1 Flow-chart of the proposed algorithm REDMOFWA.

mapping explosion operator; (3) hybrid mutation for adjusting the sub-tours; (4) objective-driven extending search; (5) update of the fireworks population and the external archives; and (6) selection. Among them, the gray parts are the novel strategies incorporated in REDMOFWA.

3.2 Partial mapping explosion operator

The proposed algorithm adopts the integer encoding. If an offset is produced by adding or subtracting an integer from one or more numbers, the resulting number may exceed the range of the number $[0, n]$. Therefore, the quantity of the changed numbers in the individual encoding is employed in this paper to represent the offsets generated around fireworks in the decision space. Based on the above idea, a partial mapping explosion operator is designed, where a new formula for calculating the explosion radius is adopted, and a fixed number of explosion sparks are generated by a partial mapping crossover operation. The length of the encoding fragment selected by the partial mapping crossover is determined by the obtained explosion radius.

Assume that the fireworks population size is N, the dimension of the decision variables is n, and the number of objectives is m. When calculating the explosion radius of a firework in the population, the two objective values are normalized first due to the different dimensions. Then the two normalized results of each firework are multiplied to obtain N products. Next, according to the proportion of the i-th ($i = 1, 2, \ldots, N$) product in the N products, the quantity of the numbers in the i-th firework to be changed is calculated. The formula to calculate the explosion radius is as follows:

$$M(X_i) = \prod_{s=1}^{m} \frac{f_s(X_i) - f_{s\,\min}}{f_{s\,\max} - f_{s\,\min}} \tag{10}$$

$$A_i = \left[n \cdot \frac{M(X_i) - M_{\min}}{M_{\max} - M_{\min}} \right] \tag{11}$$

where $f_s(X_i)$, $f_{s\,\max}$, and $f_{s\,\min}$ denote the s-th objective value of the i-th firework, the maximum, and the minimum values of all fireworks on the s-th objective, respectively. $M(X_i)$ is the product of the two normalized objective values of the i-th firework. $M_{\max}$ and $M_{\min}$ are the maximum and minimum values on the product of N fireworks, respectively. The explosion radius of the i-th firework is represented by A_i, and the rounding operation is denoted by $[\cdot]$. According to Eq. (11), when a firework is close to the extreme solution, i.e., one of its objective values is very small, the normalized product is also low, thus a small explosion radius is obtained. When both of the objective values are large, the normalized product is also high, so a large explosion radius is produced. When both of the objective values are compromised, the fireworks are located in the middle of the current Pareto front in the objective space. Besides, if the firework is near the origin of coordinates, it means that it is closer to the true Pareto front (minimization problem). In this case, a lower normalized product $M(X_i)$ is obtained from Eq. (10), and a smaller explosion radius is produced from Eq. (11). If the firework is far away from the true Pareto front, the normalized product is larger than the previous case and the explosion radius obtained is relatively larger. Based on the above principles, the explosion radii of different fireworks can be reasonably controlled by the presented calculation formula of radius. In detail, a fine search can be conducted in a small area around the potential fireworks that are close to the Pareto front, while an exploration in a large search range can be performed by the poor fireworks.

In order to further enhance the exploration and exploitation of the regions around the fireworks, four partial mapping explosion radii are determined for each firework based on A_i obtained from Eq. (11):

$$r_{i1} = A_i,\ r_{i2} = \left[\frac{3}{4}A_i\right],\ r_{i3} = \left[\frac{1}{2}A_i\right],\ r_{i4} = \left[\frac{1}{4}A_i\right] \tag{12}$$

Then for each firework, the distribution centers 0 in the encoding are deleted and a customer visiting sequence is obtained. Four visiting sequences derived from the remaining fireworks in the population are randomly selected, which are used to perform the partial mapping crossover operation with the current firework. The partial mapping explosion radii r_{i1}, r_{i2}, r_{i3}, and r_{i4} are regarded as the fragment lengths selected for the four crossover operations. After one crossover, two explosion sparks can be obtained. Thus, a total of eight explosion sparks are generated around one firework. Take a sequence with eight customers as an example. Implementation of the partial mapping explosion operator is shown in Fig. 2. Assume that $\boldsymbol{X}_1$ and $\boldsymbol{X}_2$ are two firework individuals; k_1, k_2, and k_3 denote the three sub-tours, respectively; $\boldsymbol{P}_1$ and $\boldsymbol{P}_2$ are the customer visiting sequences of $\boldsymbol{X}_1$ and $\boldsymbol{X}_2$; and the explosion radius (i.e., the length of the fragment chosen by the crossover) is four. A starting point is selected randomly (e.g., “4” in $\boldsymbol{P}_1$), then two fragments (“4 2 8

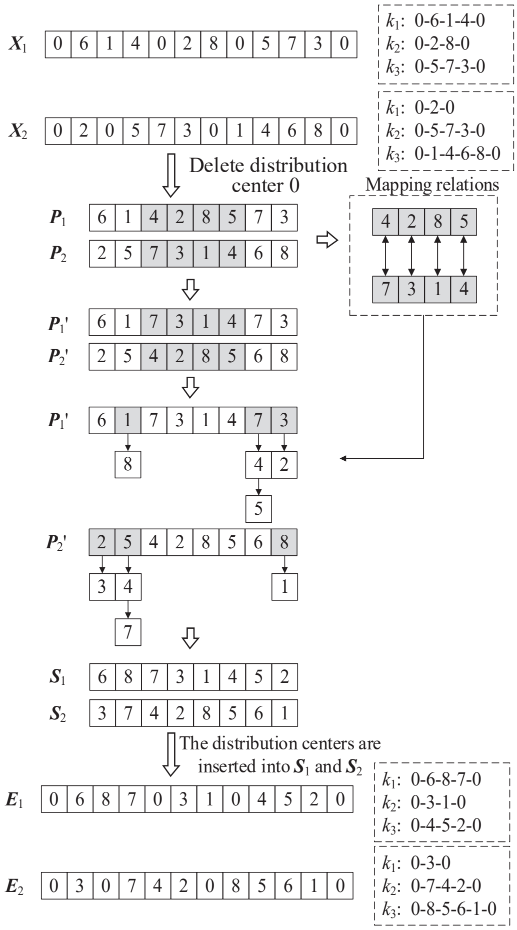

Fig. 2 Partial mapping explosion operator.

5” in $\boldsymbol{P}_1$ and “7 3 1 4” in $\boldsymbol{P}_2$) to be exchanged can be obtained according to the explosion radius. The two fragments also reflect the mapping relations of the corresponding numbers. Next, two new sequences P_1' and P_2' are created by exchanging the corresponding positions of the two fragments. After that, the numbers in the non-exchanged parts of P_1' and P_2' that are repeated with the ones in the exchanged fragments are mapped according to the mapping relations in turn, until there are no repeated numbers in the resulting customer visiting sequences $\boldsymbol{S}_1$ and $\boldsymbol{S}_2$. Finally, the distribution centers are inserted into $\boldsymbol{S}_1$ and $\boldsymbol{S}_2$ according to their locations in $\boldsymbol{X}_1$ and $\boldsymbol{X}_2$ to generate two new explosion sparks $\boldsymbol{E}_1$ and $\boldsymbol{E}_2$.

The proposed partial mapping explosion operator exchanges fragments of different lengths in the individuals by controlling the explosion radius. In this way, the information interaction among distinct individuals can be realized to varying degrees, and individuals can search in various ranges adaptively according to their own characteristics. Thus, both the global exploring and the local mining can be carried out. However, this operator only operates on the customer visiting sequence, while locations of the distribution center remain unchanged, so the population diversity is somewhat limited.

3.3 Hybrid mutation for adjusting sub-tours

Since the explosion sparks generated by the partial mapping explosion operators have the same distribution center locations as the original fireworks, the number of customers in each sub-tour of explosion sparks has not changed compared with that of fireworks, which leads to a similarity between the generated offspring and the parent individuals in the decision space, and it is easy to fall into the local optimal. In order to enhance the diversity, a hybrid mutation which adjusts the sub-tours is presented to conduct mutation on the fireworks population. Two mutation modes are included in the proposed operation. One is the sub-tour length variation operator that changes the locations of the distribution center, the other is the sub-tour load variation operator that exchanges two randomly selected points in the fireworks encoding. Take the sequence with eight customers and three available vehicles as an example, the proposed operator is illustrated in Fig. 3.

The sub-tour length variation operator randomly moves distribution centers “0” of the original firework (except “0” at the beginning and end of the encoding) to other locations of the customer visiting sequence. In

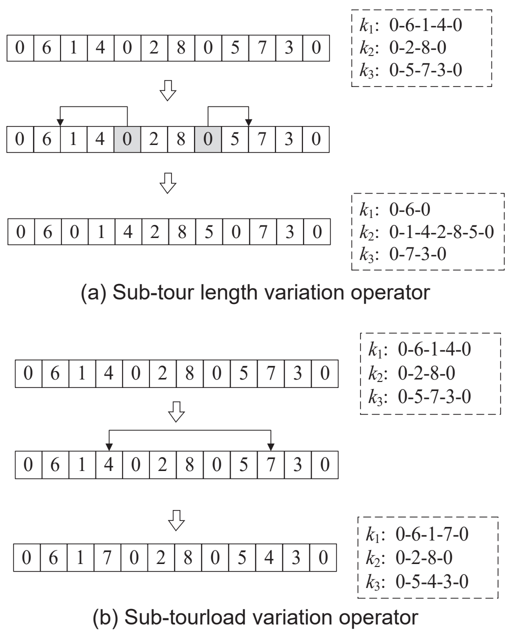

Fig. 3 Hybrid mutation for adjusting the sub-tours.

the individual of Fig. 3a, there are two “0” except the beginning and end. Insert them into the positions after customer 6 and customer 5, respectively, and the number of customers in the three sub-tours changes from three, two, and three to one, five, and two. Therefore, the number of customers, i.e., the encoding length of each sub-tour may alter after performing this variation operator. The sub-tour load variation operator randomly swaps two numbers in the firework encoding. As illustrated in Fig. 3b, customers 4 and 7 are swapped, while the encoding length of each sub-tour is not changed. Assume that the demands of customers 4 and 7 are different. Then the total customer demands of the first and third sub-tours will alter, resulting in the change of the corresponding sub-tour loads. In most cases, two customer numbers are selected to have a swap, so the length of each sub-tour in the mutated spark is unchanged, but the load alters. In rare cases, one selected number is a distribution center, the other is a customer, then both the sub-tour length and load may have a change. If both the chosen numbers are distribution centers by chance, the mutated spark is the same as the original firework.

Each of the above two variation operators is implemented on the sub-tour of each firework, which provides a new direction for exploring the feasible region. It can also prevent the population from falling into the local optimum due to the rapid assimilation, which makes up for the lack of diversity of the partial mapping explosion operator. Since both the variation operators just move the locations of the numbers in encodings, the mutated sparks are also feasible.

3.4 Objective-driven extending search

Heuristic search methods perform a search by utilizing the heuristic information contained in the problem, so as to narrow the search, and reduce the computational cost. In order to find out the extreme region of the Pareto front and widen the spread of the front, an objective-driven extending search strategy is designed inspired by the idea of heuristic search. Considering the two optimization objectives of the low-carbon VRP, carbon emissions and travel time of the vehicle in each path segment are employed as the heuristic information here. A certain sub-tour in the encoding is reordered based on the heuristic information to decrease the corresponding objective value. Take the sequence with eight customers and three vehicles as an example, and the objective-driven extending search is shown in Fig. 4. Figure 4a gives the extending search driven by the

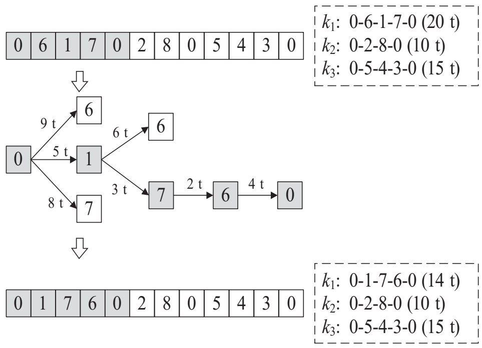

(a) Extending search driven by the carbon emissions of the path segments

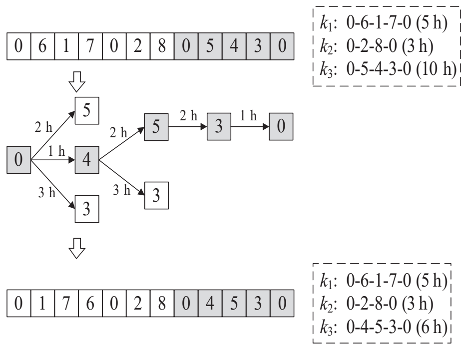

(b) Extending search driven by the travel time of the path segments

Fig. 4 Objective-driven extending search.

carbon emissions. The numbers next to the arrows and those in the parentheses of the dotted boxes denote the carbon emissions of the corresponding path segments and the total carbon emissions of the sub-tour, respectively. First, a sub-tour (0-6-1-7-0) is selected uniformly at random. Then the distribution center 0 is set as the starting point, and the customer number 1 corresponding to the path segment with the minimum carbon emission (5 t) in the sub-tour is chosen. Next, the customer 1 just selected is regarded as the new starting point, and the next visiting point is determined from the remaining customers of the sub-tour based on the carbon emission. This process iterates until the current sub-tour has been totally reordered. Finally, the obtained new sub-tour is put back into the original individual encoding. The extending search driven by the travel time is illustrated in Fig. 4b. Similar operations to those of Fig. 4a are performed except that the travel time of the path segment is adopted instead of the carbon emission. Note that the presented extending search is only carried out on the non-dominated individuals among the explosion sparks and mutated sparks, with the aim of mining their neighborhood so that better individuals can be produced.

Through the proposed objective-driven extending search, the performance of the obtained individual on at least one objective is improved. This strategy enhances the fine search for the elite individuals, which can quickly locate the region with better objective values at the early stage of the iterations, and gradually extend the distribution of the Pareto front to the extreme values. As a result, the searching efficiency of the algorithm is greatly improved and the spread of the obtained Pareto front is guaranteed.

3.5 Detailed implementation of the algorithm

The pseudo-code of the proposed algorithm REDMOFWA for solving the low-carbon VRP model is given in Algorithm 1.

Algorithm 1 A region enhanced discrete multi-objective fireworks algorithm (REDMOFWA)

Input: *N*—population size, *n*—dimensions of decision variables, *K*—the number of available vehicles, L_{max}—the maximum archive size, Eva_{max}—the maximum number of objective evaluations

Output: *archive*—the external set, *archive_obj*—the objective vectors of archive

The fireworks population *POP* with the size of N is randomly initialized and the objective vectors *POP_obj* are evaluated.

$NDS \leftarrow \varnothing$, $archive \leftarrow POP$, $Eva \leftarrow N$

while $Eva <= Eva_{max}$ **do**

 The explosion spark population *EPOP* is generated by performing the partial mapping explosion ex operator on *POP*.

 The mutated spark population *GPOP* is produced by conducting the hybrid mutationon *POP*.

 NDS←The non-dominated solutions in $EPOP \cup GPOP$.

 The extending spark population *SPOP* is obtained by performing the objective-driven extending search on *NDS*.

 $Eva \leftarrow Eva + |EPOP| + |GPOP| + |SPOP|$.

 POP is updated by *NDS* and *SPOP* based on the notion of Pareto dominance.

 archive is updated by *NDS* and *SPOP* based on the notion of ε dominance[36].

 While $|archive| > L_{max}$ **do**

  The individual with the smallest crowding distance is deleted from *archive*.

 $N/2$ individuals are selected from *archive* and *POP* randomly to form the population *NPOP* in the next generation, respectively. If $|archive| < N/2$, individuals in *POP* will be used to supplement. One individual is randomly selected from *NPOP*, and a cyclic shift is performed on other individuals in *NPOP* whose similarities to the selected individual are higher than 80%.

 $POP \leftarrow NPOP$.

Output *archive*, *archive_obj*.

4 Experimental Studies

In this paper, MATLAB R2019a software is used. All the experiments are performed on a computer with Intel(R)Core(TM)i5-10210U, CPU@1.60GHz, and 12G operating memory. Two groups of experiments are carried out: (1) validating the effectiveness of the three novel strategies; and (2) verifying the overall performance of the proposed algorithm REDMOFWA by comparing it with four state-of-the-art algorithms.

The parameter settings of REDMOFWA are set as follows: the population size N is set to 10, and the maximum archive size L_{max} is set to 100. 30 independent runs of each comparison algorithm are replicated on each problem instance, and the maximum number of objective vector evaluations Eva_{max} in each run is set to 50 000. Two metrics normally utilized in multi-objective optimization are adopted to evaluate the performance of the algorithms, which are named inverted generational distance (IGD)[37] and hypervolume (HV)[38]. A smaller IGD indicates better convergence and diversity performance of the obtained Pareto front. A larger HV shows better convergence and spread performance of the evolved Pareto front. Since the true Pareto front of the low-carbon VRP is unknown, the reference Pareto front used in IGD is obtained by combining all the Pareto fronts produced during all the independent runs applying all the comparison algorithms, and determining the non-dominated individuals from them. The worst value on each objective of all the non-dominated solutions found by the comparison algorithms is determined. Then the reference point used to calculate HV is acquired by multiplying each worst value by 1.5.

4.1 Instance generation

Nine instances with increasing scales are selected from the commonly used VRP test sets, including set A, set B, set P, and set E[39]. The number of customers, number of available vehicles, and demand of each customer are different from each other in the nine instances. The name of each instance consists of the set name, number of customers, and number of procurable vehicles. The maximum vehicle capacity in each instance is set as the sum of the demands required by all customers, so that all solutions created during the optimization will not violate the vehicle capacity constraint. In each instance, it is assumed that the speed at which the vehicle travels from customer i to customer j is different from that from j to i. A square matrix with the dimension of (n+1) is randomly constructed to represent the driving speed between any two points of the locations numbered 0−n. All the driving speeds take the value between 50−80 km/h. In the nine instances, the parameter settings of the low-carbon VRP model are listed in Table 1.

4.2 Validating the effectiveness of the three novel strategies

With the aim of validating the effectiveness of the three new strategies presented in Sections 3.2−3.4, each of them is substituted by an existing strategy or deleted from the algorithm. The partial mapping explosion operator of the proposed algorithm REDMOFWA is replaced by the explosion operator of the discrete fireworks algorithm DMOFWA in Ref. [40], and the resulting algorithm is denoted as REDMOFWA-E. The hybrid mutation for adjusting the sub-tours is replaced by the mutation operator of the discrete fireworks algorithm DFWA-TSP in Ref. [41], obtaining the algorithm REDMOFWA-M. The objective-driven extending search is deleted from REDMOFWA, and the algorithm after deletion is named REDMOFWA-O. The IGD and HV values of all the comparison algorithms on the nine instances with different scales are shown in Table 2, where mean and std represent the average and standard deviation of the metrics, respectively, and the best value is in bold. To significantly compare the algorithms, the Wilcoxon rank sum tests with the significance level of 0.05 are performed, where "+", "−", and "=" mean that the proposed algorithm is significance better than, worse than, or equal to the comparison algorithms, respectively.

Table 1 Parameter settings in the low-carbon VRP model.

Parameter symbol	Parameter value
a	0 m/s^2
C_d	0.7
A	5 m^2
ρ	1.204 kg/m^3
θ	0
w	10 t
FE	2.621×10^{-6} t/L

4.3 Validating the overall performance of the proposed algorithm

In order to verify the overall performance of REDMOFWA, two representative multi-objective optimization algorithms that are Green Vehicle Routing Problem (G-VRP)[21] and Bi-objective NSGA-II[6]

Table 2 Comparison results on validating the effectiveness of the three novel strategies.

Instance	IGD mean (std)				HV mean (std)			
	REDMOFWA	REDMOFWA-E	REDMOFWA-M	REDMOFWA-O	REDMOFWA	REDMOFWA-E	REDMOFWA-M	REDMOFWA-O
P-n19-k2	2.03×10^{-2} (5.69×10^{-3})	2.29×10^{-2} = (5.87×10^{-3})	3.22×10^{-2} + (1.28×10^{-2})	**1.77×10^{-2} =** **(4.34×10^{-3})**	**8.24×10^{-1}** **(1.70×10^{-3})**	8.19×10^{-1} = (3.29×10^{-3})	8.15×10^{-1} + (5.74×10^{-3})	8.21×10^{-1} = (3.44×10^{-3})
E-n22-k4	**9.31×10^{-3}** (1.67×10^{-3})	1.16×10^{-2} + **(1.40×10^{-3})**	3.86×10^{-2} + (1.37×10^{-2})	1.20×10^{-2} + (3.21×10^{-3})	**6.09×10^{-1}** **(2.06×10^{-3})**	6.08×10^{-1} + (2.25×10^{-3})	5.51×10^{-1} + (2.34×10^{-2})	6.06×10^{-1} + (4.10×10^{-3})
A-n34-k5	4.37×10^{-2} (9.49×10^{-3})	**4.01×10^{-2} =** **(7.34×10^{-3})**	7.69×10^{-2} + (2.69×10^{-2})	9.98×10^{-2} + (2.86×10^{-2})	**6.45×10^{-1}** **(7.92×10^{-3})**	6.32×10^{-1} = (1.06×10^{-2})	5.87×10^{-1} + (2.50×10^{-2})	5.70×10^{-1} + (2.61×10^{-2})
A-n44-k6	4.73×10^{-2} (1.34×10^{-2})	**4.26×10^{-2} =** **(1.06×10^{-2})**	7.71×10^{-2} + (1.74×10^{-2})	8.47×10^{-2} + (1.57×10^{-2})	**7.05×10^{-1}** **(7.60×10^{-3})**	6.94×10^{-1} + (1.62×10^{-2})	6.42×10^{-1} + (2.52×10^{-2})	6.32×10^{-1} + (2.09×10^{-2})
A-n54-k7	3.75×10^{-2} (1.16×10^{-2})	**3.63×10^{-2} =** **(8.43×10^{-3})**	7.30×10^{-2} + (1.45×10^{-2})	9.46×10^{-2} + (1.77×10^{-2})	**7.16×10^{-1}** **(1.04×10^{-2})**	7.03×10^{-1} = (1.43×10^{-2})	6.48×10^{-1} + (1.85×10^{-2})	6.34×10^{-1} + (1.89×10^{-2})
B-n64-k9	**4.09×10^{-2}** (1.66×10^{-2})	4.16×10^{-2} + (1.20×10^{-2})	9.14×10^{-2} + **(1.06×10^{-2})**	9.41×10^{-2} + (1.83×10^{-2})	**7.52×10^{-1}** (2.14×10^{-2})	7.36×10^{-1} + (2.48×10^{-2})	6.59×10^{-1} + **(1.86×10^{-2})**	6.54×10^{-1} + (2.09×10^{-2})
E-n76-k8	**5.04×10^{-2}** (1.33×10^{-2})	5.44×10^{-2} + **(1.33×10^{-2})**	9.92×10^{-2} + (2.21×10^{-2})	1.27×10^{-1} + (1.83×10^{-2})	**7.02×10^{-1}** (1.47×10^{-2})	7.00×10^{-1} = (1.82×10^{-2})	6.21×10^{-1} + (2.34×10^{-2})	6.10×10^{-1} + **(1.43×10^{-2})**
A-n80-k10	**4.19×10^{-2}** (1.39×10^{-2})	4.44×10^{-2} = **(9.32×10^{-3})**	7.34×10^{-2} + (1.65×10^{-2})	1.09×10^{-1} + (1.57×10^{-2})	**7.09×10^{-1}** **(1.31×10^{-2})**	7.03×10^{-1} = (1.37×10^{-2})	6.49×10^{-1} + (1.71×10^{-2})	6.21×10^{-1} + (1.42×10^{-2})
E-n101-k8	5.31×10^{-2} **(1.07×10^{-2})**	**4.17×10^{-2} −** (1.23×10^{-2})	9.55×10^{-2} + (1.90×10^{-2})	1.61×10^{-1} + (1.96×10^{-2})	7.06×10^{-1} **(1.26×10^{-2})**	**7.22×10^{-1}−** (1.58×10^{-2})	6.61×10^{-1} + (1.56×10^{-2})	6.13×10^{-1} + (1.49×10^{-2})
Total +/=/−	−	3/5/1	9/0/0	8/1/0	−	3/5/1	9/0/0	8/1/0

designed for solving the low-carbon VRP are selected as comparison algorithms. Besides, with the aim of validating the effectiveness of the multi-objective handling method in REDMOFWA, its framework for handling multiple objectives is replaced by that of the classical multi-objective metaheuristic algorithms NSGA-II[7] and Strength Pareto Evolutionary Algorithm 2 (SPEA2)[42], respectively. In this way, two additional comparison algorithms denoted as REDMOFWA-N and REDMOFWA-S are obtained, in which the encoding and the three novel strategies remain unchanged. As REDMOFWA, REDMOFWA-N, and REDMOFWA-S are fireworks algorithms, the population size takes a small value of 10, while the population size of G-VRP and Bi-objective NSGA-II (BiNSGA-II) is set to 100 as in the original literature. Other parameters in the comparison algorithms are the same as those in the original literature. The same random initialization methods are adopted in the five algorithms, and the comparison results on nine instances with different scales are shown in Table 3.

It can be seen from Table 3 that compared with the four comparison algorithms, the mean and standard deviation of the IGD values produced by REDMOFWA are optimal in seven of the nine instances. REDMOFWA obtains the best mean and standard deviation of HV in nine and five of the nine instances, respectively. Wilcoxon rank sum test results show that REDMOFWA is significantly better than the four comparison algorithms with both IGD and HV in most cases. The above results indicate that the proposed algorithm is able to provide a Pareto front with good convergence, a unform distribution, and a wide spread for the low-carbon VRP. Furthermore, it shows a promising scalability to the problem scales. The reason for the good performance of REDMOFWA is the coordination of the three new strategies. The partial mapping explosion operator adjusts the searching range of each firework adaptively by controlling the explosion radius, which realizes the information interaction among different individuals and speeds up the convergence. Population diversity is enhanced by the hybrid mutation for adjusting the sub-tours, which prevents the population from falling into the local optimum. Moreover, the objective-driven extending search is adopted to gradually extend the distribution of the Pareto front to the extreme values and widen the spread of the Pareto front. The three strategies complement each other and achieve a global search in the decision space as well as a fine mining

Table 3 Comparison results of REDMOFWA and four representative algorithms.

Instance	IGD mean (std)					HV mean (std)				
	REDMOFWA	REDMOFWA-N	BiNSGA-II	REDMOFWA-S	G-VRP	REDMOFWA	REDMOFWA-N	BiNSGA-II	REDMOFWA-S	G-VRP
P-n19-k2	2.03×10^{-2} (**5.69×10^{-3}**)	5.33×10^{-2} + (1.89×10^{-2})	**1.90×10^{-2} =** (6.30×10^{-3})	3.63×10^{-2} = (8.20×10^{-3})	2.78×10^{-1} = (3.07×10^{-2})	**8.24×10^{-1}** (**1.70×10^{-3}**)	8.13×10^{-1} + (7.05×10^{-3})	8.20×10^{-1} + (3.38×10^{-3})	8.17×10^{-1} = (4.02×10^{-3})	7.05×10^{-1} = (8.68×10^{-3})
E-n22-k4	**9.31×10^{-3}** (**1.67×10^{-3}**)	5.35×10^{-2} + (1.01×10^{-2})	1.44×10^{-2} + (4.57×10^{-3})	3.07×10^{-2} + (6.00×10^{-3})	1.69×10^{-1} + (1.08×10^{-2})	**6.09×10^{-1}** (**2.06×10^{-3}**)	5.79×10^{-1} + (8.41×10^{-3})	6.03×10^{-1} + (9.91×10^{-3})	5.93×10^{-1} + (6.16×10^{-3})	4.11×10^{-1} + (1.25×10^{-2})
A-n34-k5	**4.37×10^{-2}** (**9.49×10^{-3}**)	1.02×10^{-1} + (2.42×10^{-2})	4.90×10^{-2} = (1.55×10^{-2})	7.50×10^{-2} + (1.81×10^{-2})	5.07×10^{-1} + (1.00×10^{-1})	**6.45×10^{-1}** (**7.92×10^{-3}**)	5.89×10^{-1} + (2.00×10^{-2})	6.19×10^{-1} = (1.69×10^{-2})	6.02×10^{-1} + (1.46×10^{-2})	2.06×10^{-1} + (1.51×10^{-2})
A-n44-k6	4.73×10^{-2} (**1.34×10^{-2}**)	1.10×10^{-1} + (2.50×10^{-2})	**4.53×10^{-2} =** (1.34×10^{-2})	7.59×10^{-2} + (1.63×10^{-2})	5.13×10^{-1} + (7.73×10^{-2})	**7.05×10^{-1}** (**7.60×10^{-3}**)	6.49×10^{-1} + (1.65×10^{-2})	6.79×10^{-1} = (1.63×10^{-2})	6.62×10^{-1} + (1.71×10^{-2})	2.84×10^{-1} + (**1.49×10^{-2}**)
A-n54-k7	**3.75×10^{-2}** (**1.16×10^{-2}**)	1.29×10^{-1} + (3.17×10^{-2})	5.96×10^{-2} + (1.77×10^{-2})	9.36×10^{-2} + (1.69×10^{-2})	5.14×10^{-1} + (1.22×10^{-1})	**7.16×10^{-1}** (**1.04×10^{-2}**)	6.33×10^{-1} + (2.00×10^{-2})	6.71×10^{-1} + (1.83×10^{-2})	6.54×10^{-1} + (1.17×10^{-2})	2.39×10^{-1} + (1.18×10^{-2})
B-n64-k9	**4.09×10^{-2}** (1.66×10^{-2})	1.28×10^{-1} + (3.66×10^{-2})	6.73×10^{-2} + (**1.34×10^{-2}**)	9.51×10^{-2} + (1.87×10^{-2})	5.21×10^{-1} + (1.15×10^{-1})	**7.52×10^{-1}** (2.14×10^{-2})	6.52×10^{-1} + (2.71×10^{-2})	6.88×10^{-1} + (1.59×10^{-2})	6.69×10^{-1} + (2.02×10^{-2})	2.49×10^{-1} + (**1.54×10^{-2}**)
E-n76-k8	**5.04×10^{-2}** (**1.33×10^{-2}**)	1.76×10^{-1} + (4.61×10^{-2})	7.60×10^{-2} + (1.88×10^{-2})	1.26×10^{-1} + (2.29×10^{-2})	4.86×10^{-1} + (4.30×10^{-2})	**7.02×10^{-1}** (1.47×10^{-2})	6.11×10^{-1} + (2.02×10^{-2})	6.58×10^{-1} + (1.72×10^{-2})	6.27×10^{-1} + (1.56×10^{-2})	2.02×10^{-1} + (**7.24×10^{-3}**)
A-n80-k10	**4.19×10^{-2}** (**1.39×10^{-2}**)	1.53×10^{-1} + (3.92×10^{-2})	6.37×10^{-2} + (2.14×10^{-2})	9.70×10^{-2} + (1.83×10^{-2})	4.74×10^{-1} + (7.29×10^{-2})	**7.09×10^{-1}** (1.31×10^{-2})	6.22×10^{-1} + (2.35×10^{-2})	6.70×10^{-1} + (1.18×10^{-2})	6.48×10^{-1} + (1.22×10^{-2})	2.58×10^{-1} + (**1.16×10^{-2}**)
E-n101-k8	**5.31×10^{-2}** (1.07×10^{-2})	1.62×10^{-1} + (2.89×10^{-2})	9.03×10^{-2} + (1.90×10^{-2})	1.39×10^{-1} + (2.19×10^{-2})	4.03×10^{-1} + (**2.82×10^{-16}**)	**7.06×10^{-1}** (1.26×10^{-2})	6.26×10^{-1} + (1.92×10^{-2})	6.76×10^{-1} + (1.51×10^{-2})	6.46×10^{-1} + (**1.19×10^{-2}**)	2.52×10^{-1} + (1.28×10^{-2})
Total +/=/−	−	9/0/0	6/3/0	8/1/0	8/1/0	−	9/0/0	7/2/0	8/1/0	8/1/0

around the elite individuals. In this manner, the proposed algorithm can make a good balance between exploration and exploitation so that a wide spread of non-dominated solutions that are close to the reference Pareto front are produced.

The convergence curves of IGD and HV produced by the five algorithms with the number of objective evaluations on instance E-n76-k8 are shown in Fig. 5, from which the convergence speed and convergence accuracy of the algorithms can be visually observed. IGD and HV values are sampled every 500 times of the objective vector evaluations, so a total of 100 data points exist in a convergence curve. According to the curves, it is obvious that compared with the other four algorithms, REDMOFWA has a better convergence accuracy and a higher convergence speed on E-n76-k8. Similar results can be obtained from other instances.

5 Conclusion

Three main contributions of this work are listed as follows: (1) A constrained multi-objective optimization model for the low-carbon VRP is established, which minimizes both the total carbon emissions and the longest sub-tour time. (2) A region enhanced discrete multi-objective fireworks algorithm, named REDMOFWA, is designed to solve the low-carbon VRP. First of all, the information interaction between fireworks individuals is enhanced through the partial mapping explosion operator to improve the search efficiency. In addition, the hybrid mutation for adjusting the length and load of the sub-tours is applied to increase the diversity of the population and to obtain the approximate Pareto front of low carbon VRP as accurate and uniform as possible. Finally, the objective-driven extending search operator is conducted to searching the extreme solutions, which can improve the convergence and widen the spread of the Pareto front of the algorithm. And (3) a series of experiments are conducted to examine the strategies effectiveness and overall performance of REDMOFWA. Compared with four state-of-the-art algorithms in nine instances, the proposed algorithm REDMOFWA achieves a significant superiority for solving the low-carbon VRP in terms of convergence, diversity, and spread. Furthermore, REDMOFWA is scalable to the problem scales.

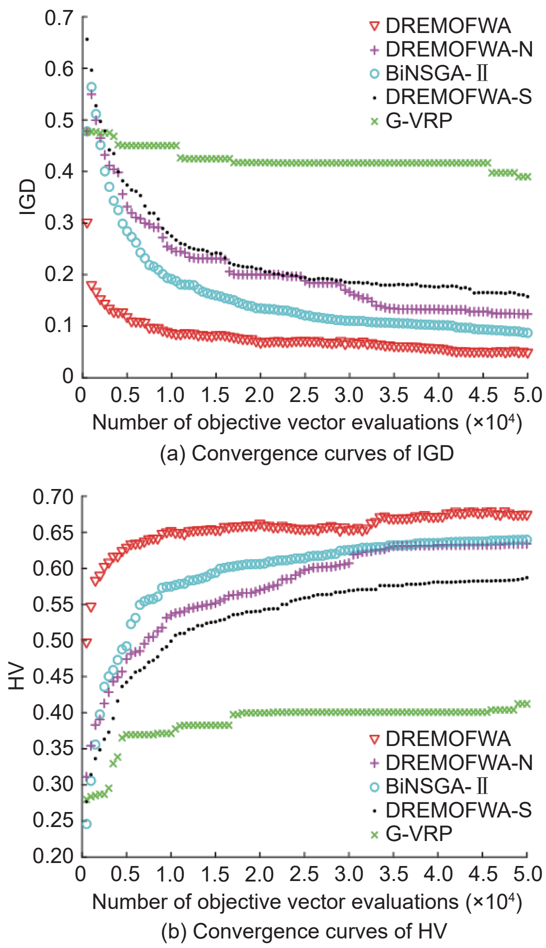

(a) Convergence curves of IGD

(b) Convergence curves of HV

Fig. 5 Convergence curves of IGD and HV produced by five algorithms on E-n76-k8.

There are still some limitations in the research of multi-objective fireworks algorithm and low-carbon VRP in this paper, which need to be further discussed and studied in future work. With model, this paper assumes that the vehicles are traveling at the same speed. However, the traffic network in real life changes dynamically, and the driving speed of the vehicle changes according to the road conditions in different time periods. Therefore, adding the actual road condition factors can make the model more suitable for the actual situation, which needs to be further studied in the future. With algorithm, the heuristic information of the problem is used to guide the algorithm search process, so that the algorithm is not universal. The next step is to investigate metaheuristics applicable to various multi-objective combinatorial optimization problems.

In addition to the method used in this paper, some other typical intelligent optimization algorithms, e.g., monarch butterfly optimization (MBO), earthworm optimization algorithm (EWA), etc., can also be adopted to solve this problem and can be used as future work for further research.

Acknowledgment

This work was supported by the Guangdong Provincial Key Laboratory (No. 2020B121201001), the National Natural Science Foundation of China (NSFC) (Nos. 61502239 and 62002148), Natural Science Foundation of Jiangsu Province of China (No. BK20150924), the Program for Guangdong Introducing Innovative and Enterpreneurial Teams (No.2017ZT07X386), Shenzhen Science and Technology Program (No. KQTD2016112514355531), and Research Institute of Trustworthy Autonomous Systems (RITAS).

References

[1] Y. Wang, S. Peng, X. Zhou, M. Mahmoudi, and L. Zhen, Green logistics location-routing problem with eco-packages, *Transportation Research Part E: Logistics and Transportation Review*, vol. 143, p. 102118, 2020.

[2] M. Asghari and S. M. J. M. Al-e-hashem, Green vehicle routing problem: A state-of-the-art review, *International Journal of Production Economics*, vol. 231, p. 107899, 2021.

[3] F. E. Zulvia, R. J. Kuo, and D. Y. Nugroho, A many-objective gradient evolution algorithm for solving a green vehicle routing problem with time windows and time dependency for perishable products, *Journal of Cleaner Production*, vol. 242, p. 118428, 2020.

[4] A. Jabbarzadeh, F. Darbaniyan, and M. S. Jabalameli, A multi-objective model for location of transfer stations: Case study in waste management system of Tehran, *Systems Engineering*, vol. 9, no. 1, pp. 109–125, 2018.

[5] T. Long and Q. S. Jia, Matching uncertain renewable supply with electric vehicle charging demand-A Bi-level event-based optimization method, *Complex System Modeling and Simulation*, vol. 1, no. 1, pp. 33–44, 2021.

[6] G. B. Dantzig and J. H. Ramser, The truck dispatching problem, *Management Science*, vol. 6, no. 1, pp. 80–91, 1959.

[7] J. Jemai, M. Zekri, and K. Mellouli, An NSGA-II algorithm for the green vehicle routing problem, in *Proc. 12th European Conference on Evolutionary Computation in Combinatorial Optimization*, Málaga, Spain, 2012, pp. 37–48.

[8] K. Deb, A. Pratap, S. Agarwal, and T. Meyarivan, A fast and elitist multiobjective genetic algorithm: NSGA-II, *IEEE Transactions on Evolutionary Computation*, vol. 6, no. 2, pp. 182–197, 2002.

[9] Z. Xu, A. Elomri, S. Pokharel, and F. Mutlu, A model for capacitated green vehicle routing problem with the time-varying vehicle speed and soft time windows, *Computers & Industrial Engineering*, vol. 137, p. 106011, 2019.

[10] J. Zhang, Y. Zhao, W. Xue, and J. Li, Vehicle routing problem with fuel consumption and carbon emission, *International Journal of Production Economics*, vol. 170, pp. 234–242, 2015.

[11] Y. Xiao, Q. Zhao, I. Kaku, and Y. Xu, Development of a fuel consumption optimization model for the capacitated vehicle routing problem, *Computers & Operations Research*, vol. 39, no. 7, pp. 1419–1431, 2012.

[12] Y. Wang, K. Assogba, J. Fan, M. Xu, Y. Liu, and H. Wang, Multi-depot green vehicle routing problem with shared transportation resource: Integration of time-dependent speed and piecewise penalty cost, *Journal of Cleaner Production*, vol. 232, pp. 12–29, 2019.

[13] D. Tayachi and H. Boukadi, A variable neighborhood search to reduce carbon dioxide emissions in the capacitated vehicle routing problem, in *Proc. 2019 6th International Conference on Control, Decision and Information Technologies* (*CoDIT*), Paris, France, 2019, pp. 297–301.

[14] R. Moghdani, K. Salimifard, E. Demir, and A. Benyettou, The green vehicle routing problem: A systematic literature review, *Journal of Cleaner Production*, vol. 279, p. 123691, 2021.

[15] X. Han, Y. Han, Q. Chen, J. Li, H. Sang, Y. Liu, Q. Pan, and Y. Nojima, Distributed flow shop scheduling with sequence-dependent setup times using an improved iterated greedy algorithm, *Complex System Modeling and Simulation*, vol. 1, no. 3, pp. 198–217, 2021.

[16] F. Zhao, S. Di, J. Cao, J. Tang, and Jonrinaldi, A novel cooperative multi-stage hyper-heuristic for combination optimization problems, *Complex System Modeling and Simulation*, vol. 1, no. 2, pp. 91–108, 2021.

[17] W. Zhang, W. Hou, C. Li, W. Yang, and M. Gen, Multidirection update-based multiobjective particle swarm optimization for mixed no-idle flow-shop scheduling problem, *Complex System Modeling and Simulation*, vol. 1, no. 3, pp. 176–197, 2021.

[18] H. Lu, S. Yang, M. Zhao, and S. Cheng, Multi-robot indoor environment map building based on multi-stage optimization method, *Complex System Modeling and Simulation*, vol. 1, no. 2, pp. 145–161, 2021.

[19] W. Gong, Z. Liao, X. Mi, L. Wang, and Y. Guo, Nonlinear equations solving with intelligent optimization algorithms: A survey, *Complex System Modeling and Simulation*, vol. 1, no. 1, pp. 15–32, 2021.

[20] X. Ge, R. Wu, amd H. Rabitz, Optimization landscape of quantum control systems, *Complex System Modeling and Simulation*, vol. 1, no. 2, pp. 77–90, 2021.

[21] P. R. De Oliveira Da Costa, S. Mauceri, P. Carroll, and F. Pallonetto, A genetic algorithm for a green vehicle routing problem, *Electronic Notes in Discrete Mathematics*, vol. 64, pp. 65–74, 2018.

[22] K. Zhang, B. Qiu, and D. Mu, Low-carbon logistics distribution route planning with improved particle swarm

optimization algorithm, in *Proc. 2016 International Conference on Logistics, Informatics and Service Science* (*LISS*), Sydney, Australia, 2016, pp. 1–4.

[23] L. B. Pulido-Gaytan, A. Tchernykh, S. Nesmachnow, A. Cristóbal-Salas, A. Avetisyan, H. E. C. Barrera, and C. J. B. Hernandez, Multi-objective optimization of vehicle routing with environmental penalty, in *Proc. 10th International Conference on Supercomputing*, Monterrey, Mexico, 2019, pp. 147–162.

[24] Y. Li, H. Soleimani, and M. Zohal, An improved ant colony optimization algorithm for the multi-depot green vehicle routing problem with multiple objectives, *Journal of Cleaner Production*, vol. 227, pp. 1161–1172, 2019.

[25] E. Jabir, V. V. Panicker, and R. Sridharan, Design and development of a hybrid ant colony-variable neighbourhood search algorithm for a multi-depot green vehicle routing problem, *Transportation Research Part D: Transport and Environment*, vol. 57, pp. 422–457, 2017.

[26] Y. Tan and Y. Zhu, Fireworks algorithm for optimization, in *Proc. First International Conference on Advances in Swarm intelligence*, Beijing, China, 2010, pp. 355–364.

[27] J. Ji, H. Xiao, and C. Yang, HFADE-FMD: A hybrid approach of fireworks algorithm and differential evolution strategies for functional module detection in protein-protein interaction networks, *Applied Intelligence*, vol. 51, pp. 1118–1132, 2021.

[28] X. Liu and X. Qin, A neighborhood information utilization fireworks algorithm and its application to traffic flow prediction, *Expert Systems with Applications*, vol. 183, p. 115189, 2021.

[29] M. Zare, M. R. Narimani, M. Malekpour, R. Azizipanah-Abarghooee, and V. Terzija, Reserve constrained dynamic economic dispatch in multi-area power systems: An improved fireworks algorithm, *International Journal of Electrical Power & Energy Systems*, vol. 126, p. 106579, 2021.

[30] Y. -J. Zheng, Q. Song, and S. -Y. Chen, Multiobjective fireworks optimization for variable-rate fertilization in oil crop production, *Applied Soft Computing*, vol. 13, no. 11, pp. 4253–4263, 2013.

[31] L. Liu, S. Zheng, and Y. Tan, S-metric based multi-objective fireworks algorithm, in *Proc. 2015 IEEE Congress on Evolutionary Computation* (*CEC*), Sendai, Japan, 2015, pp. 1257–1264.

[32] S. I. Bejinariu, H. Costin, F. Rotaru, R. Luca, and C. Niţă, Fireworks algorithm based single and multi-objective optimization, *Bulletin of the Polytechnic Institute of IASI, Automatic Control and Computer Science*, vol. 62, no. 66, pp. 19–34, 2016.

[33] X. Chen, C. Shi, A. Zhou, S. Xu, and B. Wu, A hybrid replacement strategy for MOEA/D, in *Proc. 13th International Conference on Bio-Inspired Computing: Theories and Applications*, Beijing, China, 2018, pp. 246–262.

[34] T. Zhang, G. Liu, Q. Yue, X. Zhao, and M. Hu, Using firework algorithm for multi-objective hardware/software partitioning, *IEEE Access*, vol. 7, pp. 3712–3721, 2018.

[35] H. L. Tang, H. S. Tang, and X. Zhu, Research on low-carbon vehicle routing problem based on modified ant colony algorithm, *Chinese Journal of Management Science*, vol. 29, no. 7, pp. 118–127, 2021.

[36] K. Deb, M. Mohan, and S. Mishra, Towards a quick computation of well-spread pareto-optimal solutions, in *Proc. 2nd International Conference on Evolutionary Multi-Criterion Optimization*, Faro, Portugal, 2003, pp. 222–236.

[37] Y. Sun, G. G. Yen, and Z. Yi, IGD indicator-based evolutionary algorithm for many-objective optimization problems, *IEEE Transactions on Evolutionary Computation*, vol. 23, no. 2, pp. 173–187, 2019.

[38] H. K. Singh, Understanding hypervolume behavior theoretically for benchmarking in evolutionary multi/many-objective optimization, *IEEE Transactions on Evolutionary Computation*, vol. 24, no. 3, pp. 603–610, 2020.

[39] The VRP Web, http://www.bernabe.dorronsoro.es/vrp/, 2022.

[40] L. He, W. Li, Y. Zhang, and Y. Cao, A discrete multi-objective fireworks algorithm for flowshop scheduling with sequence-dependent setup times, *Swarm and Evolutionary Computation*, vol. 51, p. 100575, 2019.

[41] N. H. Abdulmajeed and M. Ayob, A firework algorithm for solving capacitated vehicle routing problem, *International Journal of Advancements in Computing Technology*, vol. 6, no. 1, p. 79, 2014.

[42] E. Zitzler, M. Laumanns, and L. Thiele, SPEA2: Improving the strength pareto evolutionary algorithm, *TIK-Report*, doi: 10.3929/ethz-a-004284029.

Xuan You received the BS degree from Nanjing Institute of Technology, and the master degree from Nanjing University of Information Science and Technology, Nanjing, China, in 2018 and 2021, respectively. Her current research interests include multi-objective intelligent optimization algorithm and its application, and multi-objective intelligent optimization algorithm and its application.

Jiaqi Lu received the BS degree from Nanjing University of Information Science and Technology, Nanjing, China in 2021. She is currently pursuing the master degree at Nanjing University of Information Science and Technology, Nanjing, China. Her current research interests include genetic algorithms, intelligent optimization, and deep reinforcement learning.

Xiaoning Shen received the BEng, MEng, and PhD degrees from Nanjing University of Science and Technology in 2001, 2005, and 2008, respectively. She is currently a professor at the School of Automation, Nanjing University of Information Science and Technology, Nanjing, China. Her research is focused on computational intelligence multi-objective optimization and scheduling. She has presided over the National Natural Science Foundation Youth Project, the Jiangsu Natural Science Foundation Youth Project, and the Jiangsu University Natural Science Research Project. She has participated in 2 National Natural Science Foundation projects as the main participant.

She served as a reviewer for over 10 well-known academic journals, such as *IEEE Transactions on Cybernetics*, *IEEE Transactions on Emerging Topics in Computational Intelligence*, *Applied Soft Computing*, *Soft Computing*, *Theoretical Computing Science*, *Natural Computing*, *International Journal of Systems Science*, *Journal of Control and Decision*, *Journal of Nanjing University of Science and Technology*, *Journal of Central South University*, and so on.

Zhongpei Ge received the BS degree from Huali College Guangdong University of Technology in 2020. He is currently pursuing the master degree at Nanjing University of Information Science and Technology, Nanjing, China. He is currently engaged in the research of swarm intelligence computing and its application.

Liyan Song received the BS and MS degrees from Harbin Institute of Technology in 2009 and 2011, respectively. She received the PhD degree from the University of Birmingham (UK), working on software effort estimation (SEE) using machine learning methods. She is currently a research assistant professor (RAP) at Southern University of Science and Technology (SUSTech). Her main research interests focus on predictive software engineering including software defect prediction and software effort estimation using machine learning techniques, classical machine learning (such as Bayesian model, unsupervised machine learning, online learning, and class imbalance), and deep learning. She has published high quality papers in *TOSEM*, *FSE* , and *ICSE* in the area of software engineering, and *ACML* and *PAKDD* in the area of machine learning.